A Gyro Momentum Exchange Device for Space Vehicle Attitude Control

H. B. KENNEDY*
Northrop Space Laboratories, Hawthorne, Calif.

A gyro control device is described which may be used in attitude control systems requiring momentum exchange devices. It has been shown that the use of two single-degree-of-freedom gyros per vehicle axis permits nearly independent control of the three components of vehicle angular rate. The new controller will employ only two gyro wheels and three gimbals to effect control of the three components of vehicle angular rate. A moderate degradation of transient response is experienced, due to increased cross-coupling between vehicle axes; but, on the other hand, significant weight and volume reductions are achieved. It is shown that the gyro controller is an extremely efficient device when its energy requirements are compared to those for a flywheel controller. Digital simulation results are presented to illustrate the time response of an attitude control system employing the advanced gyro controller.

Nomenclature

XYZ = vehicle fixed axes
$X'Y'Z'$ = reference axes system
xyz = gyro axes
ω_{xyz} = inertial angular velocity of the gyro axes, rad/sec
ω_0 = vehicle orbital angular rate, rad/sec
p,q,r = components of vehicle angular rate relative to reference axes, rad/sec
$p_\epsilon,q_\epsilon,r_\epsilon$ = errors in components of vehicle angular rate, rad/sec
ψ,θ,ϕ = Euler angles between vehicle and reference axes, rad
$\epsilon\epsilon$
$\psi_\epsilon,\theta_\epsilon,\phi_\epsilon$ = errors in vehicle Euler angles, rad
A = moment of inertia of each gyro wheel about a transverse axis, slug-ft^2
C = moment of inertia of each gyro wheel about its spin axis, slug-ft^2
Ω = gyro wheel spin rate, rad/sec
$\bar{H}_g$ = angular momentum of the gyro(s), ft-lb-sec
$\bar{H}_v$ = angular momentum of the vehicle, ft-lb-sec
β^* = angle between controller resultant spin vector and vehicle $-Z$ axis, rad
α,β_1,β_2 = gyro gimbal angles, rad
γ_1,γ_2 = gyro gimbal angles in alternate mechanization of controller
λ = angle between the two gyro spin vectors, rad
λ_0 = value of λ at which controller is defined as saturated
M_x,M_y,M_z = components of moment on vehicle due to gimbal rates of one gyro, ft-lb
L_X,L_Y,L_Z = components of moment on vehicle due to reaction jets, ft-lb
M_X,M_Y,M_Z = components of moment on vehicle due to gyro controller gimbal angular rates, ft-lb
K_M = motor torque command constant, ft-lb/rad/sec
C_M = motor torque speed constant, ft-lb/rad/sec
I_a = moment of inertia of rotor, referred to gimbal shaft, slug-ft^2
I_X,I_Y,I_Z = vehicle moments of inertia, slug-ft^2
K_1,K_2,K_3 = angular error gain, rad/sec/rad
K = $[\sin\beta_1(0) - \sin\beta_2(0)]\cos\alpha(0)$ = integration constant derived in an example of vehicle-gimbal motion
k_i = gimbal rate command gains, dimensionless
$\bar{e}_X$ = unit vector along X axis, etc.
E = energy, ft-lb
T_X,T_Y,T_Z = components of impulsive torque applied to vehicle to desaturate controller, ft-lb-sec
$\mathrm{sgn}[x]$ = 1 if $x \geq 0$; -1 if $x < 0$

Subscript

c = commanded values

Introduction

ONE phase of space vehicle attitude control which has received considerable attention in the literature is that of momentum exchange devices. These devices include reaction flywheels, reaction spheres, and gyros.[1-8] The primary application for momentum exchange devices lies in the area of auxiliary torque generation; they usually are used in conjunction with reaction jets to eliminate an attitude limit cycle caused by system hardware nonlinearities. The momentum exchange system, however, also may find application as a primary means of control The torque-generating device to be used for a particular mission will depend on the magnitude of the torque required, total mission time, and the accuracy of control necessary.

In this paper a particular configuration of gyros used in a momentum exchange device is considered. It was shown in Ref. 5 that the use of two gyro wheels per vehicle axis in the proper manner led to the cancellation of the first-order cross-coupling moments. The main requirement, in addition to equal wheel momentum, was that the two gyro spin axes make equal angles with the controlled vehicle axis.

It will be shown that three-axis attitude control can be achieved with two gyro wheels instead of the usual three reaction flywheels or three pairs of gyros. In the system to be described, the gyro spin axes are allowed to assume arbitrary angles with respect to one of the vehicle axes, and the two parallel gimbal axes are allowed to precess in a plane defined by the remaining two vehicle axes. In this manner cross-coupling torques that previously were eliminated now are used to advantage. From the conservation of angular momentum point of view, the resultant angular momentum vector of the controller can be varied in magnitude and direction by reorienting the gimbals, and the vehicle must react in such a manner that the total angular momentum of the system remains constant.

The new gyro controller offers several advantages over three single-axis gyro controllers or three reaction flywheels. First, the mass of the two gyro wheels will be less than that for three single-axis controllers of either the gyro or flywheel type. Second, two spin motors and speed control circuits will be needed instead of six for the previously described gyro system.

Presented at the IAS Annual Summer Meeting, Los Angeles, Calif., June 19–22, 1962; revision received November 27, 1962. The author wishes to express appreciation to Carl Grubin, Northrop Space Laboratories, for his suggestions concerning the material in this paper.

* Staff Member, Space Defense Systems.

The reduced number of gimbals and gyro bearings will increase system reliability. Third, the new controller will require much less space than three of the single-axis gyro controllers. In addition, the gyro controller offers a significant saving in the energy required for a given vehicle maneuver as compared to that required for a flywheel controller.

The control equations for the three gimbal torquers in the new system will be more complicated than the control equation for a single-axis controller. A simple analog control computer may be required to mechanize the equations if optimum system performance is desired. This computer would consist of resolving potentiometers geared to the gimbal shafts and several amplifiers to provide summing and amplification functions. It may be possible, however, to eliminate the computer and use conventional servo techniques, at the expense of increased response time and increased cross-coupling between vehicle axes during transients.

Dynamics of the Gyro System

Equations of Motion for a Gyro and Vehicle

A convenient way to derive the dynamical equations describing the gyro controller is first to develop the equations of motion for a two-degree-of-freedom gyro mounted on a rotating vehicle. Then two such gyros may be considered which, with the proper constraints applied, lead to the desired relationships. The equations of motion for the two-degree-of-freedom gyro mounted on a rotating vehicle were derived in Ref. 5. For completeness, the derivation is repeated here.

Consider, then, a two-degree-of-freedom gyro with axes xyz and a vehicle with axes XYZ as shown in Fig. 1. Euler angles ψ, θ, ϕ describe the orientation of XYZ with respect to a reference set $X'Y'Z'$, where ψ is a rotation about Z', θ is a rotation about the vehicle Y axis, and ϕ is a rotation about the vehicle X axis. For a vehicle in a circular orbit, the X' axis is defined to be tangent to the orbital path and in the direction of travel, and the Y' axis is perpendicular to the orbital plane.

The basic equation describing the system of Fig. 1, in the absence of external torques, is

$$\bar{H}_g + \bar{H}_v = \text{const} \tag{1}$$

or

$$(d\bar{H}_g/dt)_{\text{inertial}} + (d\bar{H}_v/dt)_{\text{inertial}} = 0 \tag{2}$$

The first term in Eq. (2) is the moment acting on the gyro, and the second term is the moment acting on the vehicle. The moment $\bar{M}$ acting on the vehicle thus can be written

$$\bar{M} = -(d\bar{H}_g/dt)_{\text{inertial}} = -(d\bar{H}_g/dt)_{xyz} - \bar{\omega}_{xyz} \times \bar{H}_g \tag{3}$$

where $\bar{\omega}_{xyz}$ is the angular velocity of the gyro axes. $\bar{\omega}_{xyz}$ is the sum of the angular velocity of the reference axes, the relative angular velocity of the vehicle axes, and the angular velocity of the gyro axes relative to the vehicle axes. Thus

$$\begin{aligned}\bar{\omega}_{xyz} &= \omega_x\bar{e}_x + \omega_y\bar{e}_y + \omega_z\bar{e}_z \\ &= \dot{\beta}\bar{e}_x + \dot{\alpha}\sin\beta\bar{e}_y + \dot{\alpha}\cos\beta\bar{e}_z + \bar{\omega}_1 + \bar{\omega}_{X'Y'Z'}\end{aligned} \tag{4}$$

where $\bar{\omega}_{X'Y'Z'} = -\omega_0\bar{e}_{Y'}$ is the angular velocity of the reference axes, and

$$\bar{\omega}_1 = p\bar{e}_X + q\bar{e}_Y + r\bar{e}_Z \tag{5}$$

is the relative angular velocity of the body axes with respect to the reference axes.

To express $\bar{\omega}_{X'Y'Z'}$ and $\bar{\omega}_1$ in gyro coordinates, one needs the relationships between the sets of axes. These are

$$\begin{bmatrix}\bar{e}_X\\ \bar{e}_Y\\ \bar{e}_Z\end{bmatrix} = [L]\begin{bmatrix}\bar{e}_{X'}\\ \bar{e}_{Y'}\\ \bar{e}_{Z'}\end{bmatrix} \tag{6}$$

and

$$\begin{bmatrix}\bar{e}_x\\ \bar{e}_y\\ \bar{e}_z\end{bmatrix} = [N]\begin{bmatrix}\bar{e}_X\\ \bar{e}_Y\\ \bar{e}_Z\end{bmatrix} \tag{7}$$

where

$$\begin{aligned}L &= \begin{bmatrix}\cos\theta\cos\psi & \cos\theta\sin\psi & -\sin\theta\\ \sin\theta\sin\phi\cos\psi - \cos\phi\sin\psi & \sin\phi\sin\theta\sin\psi + \cos\phi\cos\psi & \sin\phi\cos\theta\\ \cos\phi\sin\theta\cos\psi + \sin\phi\sin\psi & \cos\phi\sin\theta\sin\psi - \sin\phi\cos\psi & \cos\phi\cos\theta\end{bmatrix}\\ &= \begin{bmatrix}l_1 & l_2 & l_3\\ m_1 & m_2 & m_3\\ n_1 & n_2 & n_3\end{bmatrix}\end{aligned}$$

and

$$N = \begin{bmatrix}\cos\alpha & -\sin\alpha & 0\\ -\sin\alpha\cos\beta & -\cos\alpha\cos\beta & -\sin\beta\\ \sin\alpha\sin\beta & \cos\alpha\sin\beta & -\cos\beta\end{bmatrix}$$

The angular momentum of the gyro is

$$\bar{H}_g = H_x\bar{e}_x + H_y\bar{e}_y + H_z\bar{e}_z = A\omega_x\bar{e}_x + A\omega_y\bar{e}_y + C(\Omega + \omega_z)\bar{e}_z \tag{8}$$

where Ω is the spin rate of the gyro wheel. Substituting Eqs. (4) and (8) into (3) gives

$$\begin{aligned}M_x &= -A\dot{\omega}_x - C\omega_y(\Omega + \omega_z) + A\omega_y\omega_z\\ M_y &= -A\dot{\omega}_y - A\omega_x\omega_z + C\omega_x(\Omega + \omega_z)\\ M_z &= -C(\Omega + \dot{\omega}_z)\end{aligned} \tag{9}$$

Since ω_z will be on the order of 10^{-1} rad/sec and Ω on the order of 10^2 rad/sec, Eq. (9) may be approximated very closely by

$$\begin{aligned}M_x &= -A\dot{\omega}_x - C\Omega\omega_y\\ M_y &= -A\dot{\omega}_y + C\Omega\omega_x\\ M_z &= -C(\Omega + \dot{\omega}_z)\end{aligned} \tag{10}$$

If the expressions for ω_x, ω_y, and ω_z obtained with the aid of Eqs. (4–7) are substituted into Eq. (10), the result will be

$$\begin{aligned}M_x \cong -C\Omega\,[&\dot{\alpha}\sin\beta + \omega_0(l_2\sin\alpha\cos\beta + m_2\cos\alpha\cos\beta + n_2\sin\beta) - (p\sin\alpha + q\cos\alpha)\cos\beta - r\sin\beta] -\\ &A(\ddot{\beta} + \dot{p}\cos\alpha - p\dot{\alpha}\sin\alpha - \dot{q}\sin\alpha - q\dot{\alpha}\cos\alpha)\end{aligned} \tag{11}$$

$$\begin{aligned}M_y \cong C\Omega[&\dot{\beta} + p\cos\alpha - q\sin\alpha - \omega_0(l_2\cos\alpha - m_2\sin\alpha)] - A[\ddot{\alpha}\sin\beta + \dot{\alpha}\dot{\beta}\cos\beta - \dot{p}\sin\alpha\cos\beta -\\ &p(\dot{\alpha}\cos\alpha\cos\beta - \dot{\beta}\sin\alpha\sin\beta) - \dot{q}\cos\alpha\cos\beta +\\ &q(\dot{\alpha}\sin\alpha\cos\beta + \dot{\beta}\cos\alpha\sin\beta) - \dot{r}\sin\beta - r\dot{\beta}\cos\beta]\end{aligned} \tag{12}$$

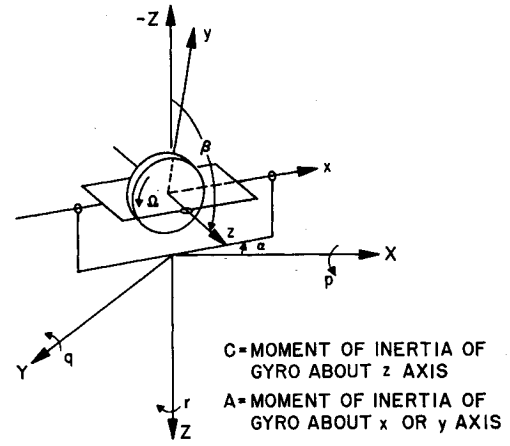

Fig. 1 Two-degree-of-freedom gyro

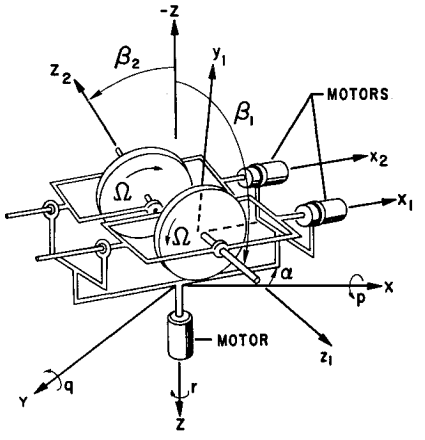

Fig. 2 Three-axis gyro controller

$$M_z \cong -C\{\dot{\Omega} + \ddot{\alpha}\cos\beta - \dot{\alpha}\dot{\beta}\sin\beta + p(\dot{\alpha}\cos\alpha\sin\beta + \dot{\beta}\sin\alpha\cos\beta) + \dot{p}\sin\alpha\sin\beta + q(\dot{\beta}\cos\alpha\cos\beta - \dot{\alpha}\sin\alpha\sin\beta) + \dot{q}\cos\alpha\sin\beta + r\dot{\beta}\sin\beta - \dot{r}\cos\beta - \omega_0[l_2(\dot{\alpha}\cos\alpha\sin\beta + \dot{\beta}\sin\alpha\cos\beta) + \dot{l}_2\sin\alpha\sin\beta + m_2(\dot{\beta}\cos\alpha\cos\beta - \dot{\alpha}\sin\alpha\sin\beta) + \dot{m}_2\cos\alpha\sin\beta + n_2\beta\sin\beta - \dot{n}_2\cos\beta]\} \quad (13)$$

where terms containing $\omega_0 p$, $\omega_0\dot{\alpha}$, and so forth were neglected in comparison to terms containing $\omega_0\Omega$. Gimbal rates may be expected to be on the order of 10^{-1} rad/sec, so that for practical purposes terms such as $\dot{p}$, $p\dot{\alpha}$, and $\dot{\alpha}\dot{\beta}$ may be neglected in favor of terms such as $\Omega\beta$, Ωp, etc. In addition, it is assumed that $\dot{\Omega} = 0$. Therefore, Eqs. (11–13), for practical purposes, reduce to

$$M_x \cong -C\Omega\{\dot{\alpha}\sin\beta + \omega_0[(l_2\sin\alpha + m_2\cos\alpha)\cos\beta + n_2\sin\beta] - (p\sin\alpha + q\cos\alpha)\cos\beta - r\sin\beta\} - A\ddot{\beta} \quad (14)$$

$$M_y \cong C\Omega[\dot{\beta} + p\cos\alpha - q\sin\alpha - \omega_0(l_2\cos\alpha - m_2\sin\alpha)] - A\ddot{\alpha}\sin\beta \quad (15)$$

$$M_z \cong -C\ddot{\alpha}\cos\beta \quad (16)$$

Terms containing gimbal accelerations are retained to facilitate the description of motor and gimbal dynamics.

Thus Eqs. (14–16) express the relationship between the moment acting on the vehicle and the angular rates of the vehicle and gimbals.

Gyro Controller Equations of Motion

The gyro controller to be described consists of a pair of two-degree-of-freedom gyros with a common second or outer gimbal. The outer gimbal axis is constrained to be parallel to the vehicle Z axis, as shown in Fig. 2. Each of the three gimbals is precessed independently by a separate torquer. The fact that the vehicle and wheel centers of gravity are not quite coincident is neglected.

The purpose of this section is to derive the equations for the moment acting on the vehicle in terms of the vehicle rates p, q, r and the gimbal angles α, β_1, β_2, and their derivatives. In addition, two examples of vehicle and gimbal motion are given, and equations are derived to determine the size of the gyro wheels in terms of the required controller capacity.

The moment acting on the vehicle due to the motion of each gyro is given by Eqs. (14–16). These components may be referred to vehicle coordinates by

$$M_X = -M_{y_1}\cos\beta_1\sin\alpha - M_{y_2}\cos\beta_2\sin\alpha + (M_{x_1} + M_{x_2})\cos\alpha + (M_{z_1}\sin\beta_1 - M_{z_2}\sin\beta_2)\sin\alpha \quad (17)$$

$$M_Y = -M_{y_1}\cos\beta_1\cos\alpha - M_{y_2}\cos\beta_2\cos\alpha - (M_{x_1} + M_{x_2})\sin\alpha + (M_{z_1}\sin\beta_1 - M_{z_2}\sin\beta_2)\cos\alpha \quad (18)$$

$$M_Z = -M_{y_1}\sin\beta_1 + M_{y_2}\sin\beta_2 - (M_{z_1}\cos\beta_1 + M_{z_2}\cos\beta_2) \quad (19)$$

It should be recognized that β_2 is measured in the opposite sense from β_1 and must be taken into account when evaluating M_{x_2}, M_{y_2}, and M_{z_2}. Substitution of Eqs. (14–16) with proper subscripts into Eqs. (17–19) yields

$$M_X = -C\Omega(\dot{\beta}_1\cos\beta_1 - \dot{\beta}_2\cos\beta_2)\sin\alpha + C\Omega(q - m_2\omega_0)(\cos\beta_1 + \cos\beta_2) - C\Omega(\dot{\alpha} - r + \omega_0 n_2)(\sin\beta_1 - \sin\beta_2)\cos\alpha - (C - A)\ddot{\alpha}(\sin\beta_1\cos\beta_1 - \sin\beta_2\cos\beta_2)\sin\alpha - A(\ddot{\beta}_1 - \ddot{\beta}_2)\cos\alpha \quad (20)$$

$$M_Y = C\Omega(\dot{\alpha} - r + \omega_0 n_2)(\sin\beta_1 - \sin\beta_2)\sin\alpha - C\Omega(\dot{\beta}_1\cos\beta_1 - \beta_2\cos\beta_2)\cos\alpha - C\Omega(\cos\beta_1 + \cos\beta_2)(p - \omega_0 l_2) - (C - A)\ddot{\alpha}(\sin\beta_1\cos\beta_1 - \sin\beta_2\cos\beta_2)\cos\alpha + A(\ddot{\beta}_1 - \ddot{\beta}_2)\sin\alpha \quad (21)$$

$$M_Z = -C\Omega(\dot{\beta}_1\sin\beta_1 + \dot{\beta}_2\sin\beta_2) + C\Omega(q - \omega_0 m_2)(\sin\beta_1 - \sin\beta_2)\sin\alpha - C\Omega(p - \omega_0 l_2)(\sin\beta_1 - \sin\beta_2)\cos\alpha + C\ddot{\alpha}(\cos^2\beta_1 + \cos^2\beta_2) + A\ddot{\alpha}(\sin^2\beta_1 + \sin^2\beta_2) \quad (22)$$

Thus, Eqs. (20–22) give the components of the moment acting on the vehicle as a function of the existing vehicle angular rate and the three gimbal angles and angular rates. If the three independent variables α, β_1, β_2 are specified properly, then the three components of the moment applied to the vehicle, and hence the vehicle angular rate, can be controlled as desired.

Two specific examples of vehicle and gimbal motion are considered. In the first example, the motion of the gimbals is prescribed as a function of time, and it is desired to find the resulting vehicle motion. Apply the initial conditions $p(0) = q(0) = r(0) = r(0) = \omega_0 = 0$, $\alpha \equiv 0$, and $\beta_1(0) = \beta_2(0) = \pi/2$ to the usual Euler equations of motion for a rigid body with Eqs. (20–22) expressing the components of the applied moment. With the stated initial conditions, it will be noted that $M_X = M_Y = 0$, and

$$M_Z = I_Z\dot{r} = -2C\Omega\dot{\beta}\sin\beta \quad (23)$$

if $\beta_1 \equiv \beta_2 \equiv \beta$. Equation (23) may be integrated, giving

$$r(t) = (2C\Omega/I_Z)\cos\beta \quad (24)$$

The result given by Eq. (24) may be obtained directly by inspection of Fig. 2. With the initial conditions given, the angular momentum of the total system is zero at $t = 0$. When the gimbals are reoriented to the angle β, the resultant controller momentum vector is $2C\Omega\cos\beta$, and the vehicle must have the angular rate $r(t)$ as given by Eq. (24) to conserve angular momentum.

Equation (24) illustrates the fact that the maximum $r(t)$ is obtained when $\beta = 0, \pi$. Thus the controller, for this special case, is saturated when the spin axes are parallel and in the

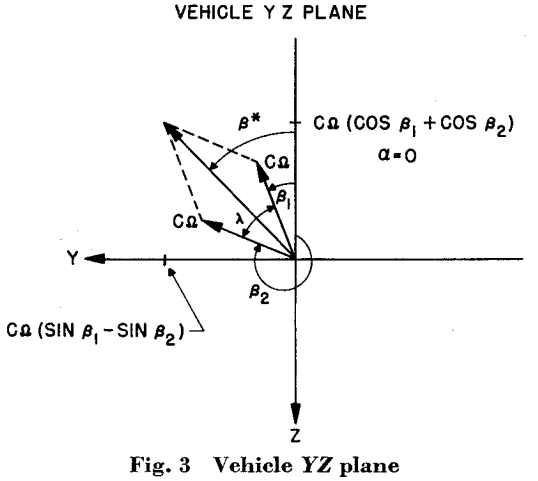

Fig. 3 Vehicle YZ plane

same sense. This is not true for the general case, since gimbal rates theoretically could become large, and hence appreciable angular momentum could be exchanged between gimbals and vehicle. High gimbal rates, as will be shown later, are undesirable from an energy point of view, and therefore the controller will be defined as saturated when the spin vectors are parallel and in the same sense.

For the second example, it is desired to investigate the effects of the orbital rate ω_0 on gimbal motion. Again, a special case will be considered, in order to make the problem tractable. The angular motion of the vehicle is prescribed as follows: $p = q = r = 0$, and Euler angles ψ, θ, ϕ are identically zero. The result of these conditions is that the vehicle has a constant angular rate $-\omega_0$ about the vehicle Y axis, and M_X, M_Y, M_Z must equal zero. It is desired to find the gimbal motion necessary to produce the given effects. If the assumption is made that terms such as $C\Omega\dot{\alpha}$ are negligible with respect to terms such as $C\Omega\dot{\alpha}$, Eqs. (20–22) give

$$(\dot{\beta}_1 \cos\beta_1 - \dot{\beta}_2 \cos\beta_2) \sin\alpha + \dot{\alpha}(\sin\beta_1 - \sin\beta_2) \cos\alpha = -\omega_0(\cos\beta_1 + \cos\beta_2)$$

$$(\beta_1 \cos\beta_1 - \dot{\beta}_2 \cos\beta_2) \cos\alpha - \dot{\alpha}(\sin\beta_1 - \sin\beta_2) \sin\alpha = 0$$

$$\beta_1 \sin\beta_1 + \dot{\beta}_2 \sin\beta_2 = -\omega_0(\sin\beta_1 - \sin\beta_2) \sin\alpha \quad (25)$$

Equations (25) may be rewritten as

$$(d/dt)\ [(\sin\beta_1 - \sin\beta_2) \sin\alpha] = -\omega_0(\cos\beta_1 + \cos\beta_2) \quad (26)$$

$$(d/dt)\ [(\sin\beta_1 - \sin\beta_2) \cos\alpha] = 0 \quad (27)$$

$$(d/dt)\ (\cos\beta_1 + \cos\beta_2) = \omega_0(\sin\beta_1 - \sin\beta_2) \sin\alpha \quad (28)$$

There are three arbitrary constants involving the three initial conditions $\alpha(0), \beta_1(0), \beta_2(0)$ associated with the solution to Eqs. (26–28). Equation (27) may be integrated directly to give

$$(\sin\beta_1 - \sin\beta_2) \cos\alpha = [\sin\beta_1(0) - \sin\beta_2(0)] \cos\alpha(0) \equiv K \quad (29)$$

Referring to Fig. 3, one sees that $C\Omega\ (\sin\beta_1 - \sin\beta_2)$ is the component of the resultant controller spin vector in the vehicle XY plane.

Next, combining Eqs. (26, 28, and 29),

$$(d^2/dt^2)(K \tan\alpha) + \omega_0^2\ (K \tan\alpha) = 0 \quad (30)$$

The solution to Eq. (30) is

$$K \tan\alpha = a \sin\omega_0 t + b \cos\omega_0 t \qquad K \neq 0 \quad (31)$$

which shows that $\tan\alpha$ is periodic in ω_0. Evaluating Eq. (31) at $t = 0$ gives $b = K \tan\alpha(0)$. Differentiating Eq. (31) and setting $t = 0$ gives $a = K\dot{\alpha}(0)/\omega_0 \cos^2\alpha(0)$. If Eqs. (26) and (29) are combined and the indicated differentiation performed, it is seen that, at $t = 0$,

$$K\dot{\alpha}(0)/\omega_0 \cos^2\alpha(0) = -[\cos\beta_1(0) + \cos\beta_2(0)] \quad (32)$$

Equation (31) then becomes

$$K \tan\alpha = -[\cos\beta_1(0) + \cos\beta_2(0)] \sin\omega_0 t + K\tan\alpha(0) \cos\omega_0 t \quad (33)$$

$$K \neq 0$$

Equation (32) indicates the required value of $\dot{\alpha}(0)$ to satisfy the constraints and initial conditions.

From Eqs. (26) and (28), it is found that

$$(\cos\beta_1 + \cos\beta_2) = K \tan\alpha(0) \sin\omega_0 t + [\cos\beta_1(0) + \cos\beta_2(0)] \cos\omega_0 t \quad (34)$$

Referring again to Fig. 3, one sees that $C\Omega(\cos\beta_1 + \cos\beta_2)$ is the $-Z$ component of the resultant spin vector.

It is interesting to note the reason for the restriction $K \neq 0$ in Eq. (33). There is a set of initial conditions for which the approximations used in obtaining Eqs. (25) are not valid. If the value of K is zero and $\cos\beta_1(0) + \cos\beta_2(0) \neq 0$, Eq. (33) is true only at $t = 0$. For all nonzero values of time α must equal $\pi/2$, implying an infinite gimbal rate $\dot{\alpha}$ at $t = 0^+$ for all $\alpha(0) \neq \pi/2$. This requirement is necessary because of the gimbal configuration and the prescribed vehicle motion. This is borne out by Eq. (32), which shows that, for $\cos^2\alpha(0) > 0$ and $\cos\beta_1(0) + \cos\beta_2(0) \neq 0$, $\dot{\alpha}(0) \to \infty$ as $K \to 0$.

One of the important considerations in this example is whether or not the controller ever becomes saturated due to the orbital rate. Therefore, the value of λ as a function of time should be investigated. Equations (29) and (34) give the components of the resultant spin vector, and if the two components are squared and added it will be seen that the magnitude is a constant, implying a constant λ. The proof is straightforward, requiring only the relation

$$1/\cos^2\alpha = 1 + \tan^2\alpha$$

The angle that the resultant spin vector makes with the $-Z$ axis, β^*, can be determined by dividing Eq. (34) by Eq. (29) to yield

$$\cot\beta^* = [\cot\beta^*\ (0)/\cos\alpha\ (0)]\cos\alpha \cos\omega_0 t + \tan\alpha\ (0) \cos\alpha \sin\omega_0 t \quad (35)$$

provided $K \neq 0$. Thus Eqs. (33) and (35) express the orientation of the resultant spin vector relative to the vehicle axes as a function of time.

Gyro Wheel Sizing

The angular momentum of each gyro wheel differs from $C\Omega$ by virtue of the gimbal rates and the body rates p, q, r. The spin rate will be several hundred radians per second, and the body rates will be only a few tenths of a radian per second in practice. It has been stated already that, for energy considerations, gimbal rates should be kept small. Therefore, for purposes of wheel sizing, the angular momentum of each wheel may be considered to be $C\Omega$. If it is desired that the controller be capable of exchanging a value of angular momentum $H_{\max}$ with the vehicle, then

$$2\ C\Omega \cos(\lambda_0/2) = H_{\max}$$

or

$$C\Omega = [H_{\max}/2 \cos(\lambda_0/2)] \quad (36)$$

In order to compare the wheel sizes of gyro and flywheel systems, let the maximum angular momentum of each flywheel be $H_{\max}/3^{1/2}$. Then it easily is shown that the momentum of one gyro wheel is related to the maximum angular momentum of one flywheel by

$$(C\Omega)_{\text{gyro}} = (3^{1/2}/2)\ (C\Omega_{\max})_{\text{flywheel}} = 0.866\ (C\Omega_{\max})_{\text{flywheel}} \quad (37)$$

Thus the mass of the two gyro wheels should be less than that of the three flywheels if the maximum rate of the flywheel is equal to the gyro wheel rate.

The gyro system has another advantage. The saturation level for the controller is $H_{\max}$, but the vector $\bar{H}_{\max}$ may have an arbitrary direction, even along one of the vehicle axes. The flywheel system has the same saturation level, but, for the case cited, the maximum along one vehicle axis is $H_{\max}/3^{1/2}$. The reaction sphere shares this advantage with the gyro controller.

Comparison of Energy Requirements for Gyro and Flywheel Systems

The maximum change in vehicle angular momentum will be attained when the gyro spin axes have been aligned, in the case of a gyro system, or when the inertia wheel reaches full speed in the case of the inertia wheel system. It is, of course, presupposed that the flywheel has a limiting speed, and that gimbal rates will be low enough so that momentum exchange between the vehicle and gimbals will be negligible. A good figure of merit for a controller is the amount of energy required

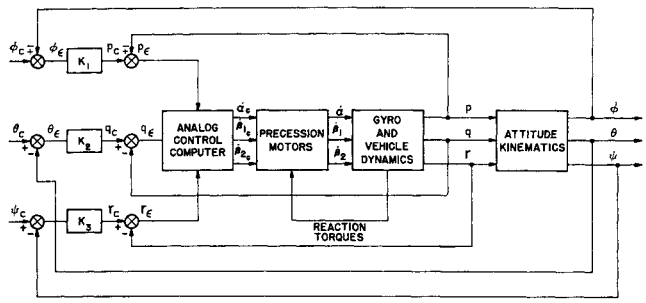

Fig. 4 Three-axis attitude control system

to accelerate the vehicle from zero to the maximum obtainable angular velocity. This energy for the gyro system will be compared with that for a flywheel system to yield a relationship between the efficiencies of the two systems in terms of system parameters.

It is apparent that there is no additional energy stored in the gyro system as a result of a gimbal reorientation if gimbal rates are zero at the end of the process. The energy actually supplied is used in accelerating the vehicle and in accelerating and decelerating the combined gimbal and rotor mass. Therefore, almost all of the energy supplied by the motor appears as kinetic energy of the vehicle. It was shown in Ref. 5, for a single vehicle axis controller, that, if the gimbal and rotor inertia could be neglected, the energy required by the gyro system is

$$E_1 = \tfrac{1}{2} I_Z r_{\max}^2 \qquad r(0) = 0 \quad (38)$$

for motion about one vehicle axis. The corresponding energy requirement for the flywheel system is

$$E_2 = \tfrac{1}{2} C_2 \Omega_{2\max}^2 + \tfrac{1}{2} I_Z r_{\max}^2 \quad (39)$$

If it is assumed that $C_1\Omega_1 = C_2\Omega_{2\max}$ (which is required for identical performance), the ratio of the energy necessary for the reaction wheel system to that for the gyro system is

$$E_2/E_1 = 1 + \Omega_{2\max}/r_{\max} \quad (40)$$

Normally the ratio of I_Z/C_2 for a flywheel system is of the order of 10^5, so that $\Omega_{2\max}/r_{\max}$ is also of the order of 10^5. This clearly demonstrates the efficiency of the gyro system. In the digital simulation section, results will be presented to demonstrate the energy requirement for the gyro system with the gimbal and rotor inertia included.

Control System Synthesis

Gimbal Control Laws

If the gyro device described in the previous section is to be used in an attitude control system, each of the gimbal angles must be specified as a function of the errors in vehicle attitude and/or angular rate. As evidenced by Eqs. (20–22), each component of the moment applied to the vehicle involves the three gimbal angles and angular rates; therefore, the three gimbal control equations, of necessity, will be coupled closely.

In order to discuss gimbal control laws, it is necessary first to define the system error information that is available to the controller. In the system to be described, it is assumed that attitude and rate sensors are used, so that errors in angular rate about each vehicle axis can be computed. Since gimbal angular rates give rise to vehicle angular acceleration, the philosophy adopted here will be to command gimbal angular rates in proportion to errors in vehicle angular rate. Thus the gimbal control laws may take the form

$$\dot{\alpha}_c = f_1 p_\epsilon + f_2 q_\epsilon + f_3 r_\epsilon \quad (41)$$

$$\dot{\beta}_{1c} = f_4 p_\epsilon + f_5 q_\epsilon + f_6 r_\epsilon \quad (41)$$

$$\dot{\beta}_{2c} = f_7 p_\epsilon + f_8 q_\epsilon + f_9 r_\epsilon \quad (43)$$

where $f_i = f_i(\alpha, \beta_1, \beta_2)$.

In Fig. 4 the attitude control system is illustrated. The author is not aware of any analytical method for determining the f_i. Hence an intuitive approach will be taken, with the realization that the results will not necessarily be optimum.

First, note that M_Z as given by Eq. (22) does not involve $\dot{\alpha}$, and involves α only in two of the undesired cross-coupling terms. Hence, let

$$f_3 = 0 \quad (44)$$

The choice of the remaining two functions in Eq. (41) can be explained by considering the expression for the resultant spin momentum,

$$\bar{H}_g' = C\Omega \sin\alpha (\sin\beta_1 - \sin\beta_2)\bar{e}_X + C\Omega \cos\alpha (\sin\beta_1 - \sin\beta_2)\bar{e}_Y - C\Omega (\cos\beta_1 + \cos\beta_2)\bar{e}_Z \quad (45)$$

Equation (45) shows that the ratio of the X and Y components of $\bar{H}_g'$ is determined by α. Since $\bar{H}_g' \cong \bar{H}_g$ (the two differ by virtue of vehicle and gimbal rates),

$$\tan\alpha \cong H_{gX}/H_{gY} \quad (46)$$

If the outer gimbal were precessed in such a manner as to force

$$\tan\alpha = I_X p_\epsilon / I_Y q_\epsilon \quad (47)$$

p_ϵ and q_ϵ could be reduced to zero simultaneously. A control law that will accomplish this is

$$\dot{\alpha}_c = -\mathrm{sgn}[\sin\beta_1 - \sin\beta_2](k_1 \cos\alpha\, p_\epsilon - k_2 \sin\alpha\, q_\epsilon) \quad (48)$$

where

$$k_1 I_Y = k_2 I_X \quad (49)$$

and

$$\mathrm{sgn}[x] = \begin{cases} 1 & x \geq 0 \\ -1 & x < 0 \end{cases}$$

The term $\mathrm{sgn}[\sin\beta_1 - \sin\beta_2]$ is necessary to resolve the 180° ambiguity in the orientation of the XY component of $\bar{H}_g'$. It is seen that, if $\dot{\alpha}_c = 0$ in Eq. (48), the result in Eq. (47) is obtained.

The task of specifying f_4 through f_9 remains. The first thought might be to make $f_i = k_i$, $i = 4$ to 9. This undoubtedly would yield a system with a satisfactory transient response for certain sets of initial conditions. For other initial conditions, however, the gimbals would precess in the wrong direction initially, and severe cross-coupling moments would result. Even if the system were stable, the transient response in such instances would be slow and energy would be wasted.

With this consideration in mind, the two remaining control equations have been chosen as

$$\dot{\beta}_{1c} = -k_3 \,\mathrm{sgn}[\cos\beta_1](\sin\alpha)p_\epsilon - k_4 \,\mathrm{sgn}[\cos\beta_1](\cos\alpha)q_\epsilon - k_5 \,\mathrm{sgn}[\sin\beta_1]\, r_\epsilon \quad (50)$$

$$\dot{\beta}_{2c} = k_6 \,\mathrm{sgn}[\cos\beta_2](\sin\alpha)p_\epsilon + k_7 \,\mathrm{sgn}[\cos\beta_2](\cos\alpha)q_\epsilon - k_8 \,\mathrm{sgn}[\sin\beta_2]r_\epsilon \quad (51)$$

If the $\sin\alpha$, $\cos\alpha$ factors were included within the brackets, i.e., $\mathrm{sgn}[\cos\beta_1 \sin\alpha]$, the equations simply would take into account the octant that the particular spin vector is in and would cause the gimbal to precess in the proper direction. If one multiplies the k's appropriately by $\sin\alpha$, $\cos\alpha$, as in Eqs. (50) and (51), the gain of the particular term will be lowered when the outer gimbal is in such a position that the controller is ineffective for that particular vehicle axis. This further reduces undesirable cross-coupling effects.

There is a relationship between the k_i which must be satisfied if the system is to perform properly. Consider a well-behaved attitude control system in which attitude errors, angular rate errors, and gimbal rates are zero at $t = 0$. Suppose that at $t = 0$ a change in attitude is commanded. For a desirable system, the attitude and rate errors should be

reduced to zero, and thus the vehicle reoriented, with the gimbals and vehicle again at rest. Therefore, in the steady state for the example cited, $\dot{\alpha}_c = \dot{\beta}_{1c} = \dot{\beta}_{2c} = 0$. From Eqs. (48, 50, and 51), this requirement gives

$$k_1 \cos\alpha\, p_\epsilon - k_2 \sin\alpha\, q_\epsilon = 0 \tag{52}$$

$$-k_3 \sin\alpha\, \mathrm{sgn}[\cos\beta_1]\, p_\epsilon - k_4 \cos\alpha\, \mathrm{sgn}[\cos\beta_1]\, q_\epsilon - k_5\, \mathrm{sgn}[\sin\beta_1]\, r_\epsilon = 0 \tag{53}$$

$$k_6 \sin\alpha\, \mathrm{sgn}[\cos\beta_2] p_\epsilon + k_7 \cos\alpha\, \mathrm{sgn}[\cos\beta_2] q_\epsilon - k_8\, \mathrm{sgn}[\sin\beta_2]\, r_\epsilon = 0 \tag{54}$$

Equations (52–54) must hold for steady-state conditions; furthermore, it is desired that the only values of p_ϵ, q_ϵ, r_ϵ satisfying these equations are $p_\epsilon = q_\epsilon = r_\epsilon = 0$. Since the three equations of interest are homogeneous, the only way to insure the desired result is to require that the determinant of Eqs. (52–54) be nonzero. This is equivalent to

$$\mathrm{sgn}[\cos\beta_1]\, \mathrm{sgn}[\sin\beta_2]\, (k_1 k_4 k_8 \cos^2\alpha + k_2 k_3 k_8 \sin^2\alpha) \neq \mathrm{sgn}[\cos\beta_2]\, \mathrm{sgn}[\sin\beta_1]\, (k_1 k_5 k_7 \cos^2\alpha + k_2 k_5 k_6 \sin^2\alpha) \tag{55}$$

Since the coefficients $\mathrm{sgn}[\cos\beta_i]\, \mathrm{sgn}[\sin\beta_j]$ may be either $+1$ or -1 and on occasion may be the same, inequality (55) leads to

$$k_8 (k_1 k_4 \cos^2\alpha + k_2 k_3 \sin^2\alpha) \neq k_5 (k_1 k_7 \cos^2\alpha + k_2 k_6 \sin^2\alpha) \tag{56}$$

Now if it is required that

$$k_4 = k_7 \qquad k_3 = k_6 \tag{57}$$

it is seen that (56) always holds if

$$k_5 \neq k_8 \tag{58}$$

thus assuring that the original requirement for a nonzero determinant always is satisfied. Equations (57) and (58) simply imply that the control laws for the inner gimbals be dissimilar.

A second set of gimbal control laws can be derived by considering a second method of mechanizing the gyro controller. One problem with the set of equations already derived is that the two inner gimbal motors do not control the magnitude and direction of the resultant controller angular momentum independently. That is, a change in one of the inner gimbal angles affects both the magnitude and the direction of the controller angular momentum.

One way to alleviate this interdependence is to add a fourth gimbal. The two inner gimbals then will be geared together and precessed differentially, with the resultant vector always perpendicular to the added gimbal. The new gimbal will be precessed relative to the outer gimbal by a second motor, while the outer gimbal will be precessed by a third motor as before. The accomplishment here is that one motor now controls the magnitude of the angular momentum of the controller.

In Fig. 5 the vector relations are illustrated for the case when $\alpha = 0$. It is seen that the two new angles γ_1, γ_2 determine the orientation and magnitude of the momentum vector. The new angles are related to β_1, β_2 by

$$\beta_1 = \gamma_2 + \gamma_1 \qquad \beta_2 = \gamma_2 - \gamma_1 \tag{59}$$

Now, if one employs the same reasoning that led to Eqs. (48, 50, and 51), a set of control equations for the new configuration results:

$$\dot{\alpha}_c = -\mathrm{sgn}[\sin\gamma_1 \cos\gamma_2]\, (k_1 \cos\alpha\, p_\epsilon - k_2 \sin\alpha\, q_\epsilon) \tag{60}$$

$$\dot{\gamma}_{1c} = -k_3\, \mathrm{sgn}[\cos\gamma_1 \cos\gamma_2] \sin\alpha\, p_\epsilon - k_4\, \mathrm{sgn}[\cos\gamma_1 \cos\gamma_2] \cos\alpha\, q_\epsilon - k_5\, \mathrm{sgn}[\sin\gamma_1 \cos\gamma_2] r_\epsilon \tag{61}$$

$$\dot{\gamma}_{2c} = k_6\, \mathrm{sgn}[\sin\gamma_1 \sin\gamma_2] \sin\alpha\, p_\epsilon + k_7\, \mathrm{sgn}[\sin\gamma_1 \sin\gamma_2] \cos\alpha\, q_\epsilon - k_8\, \mathrm{sgn}[\cos\gamma_1 \sin\gamma_2] r_\epsilon \tag{62}$$

It is not necessary actually to add the fourth gimbal to the system. Satisfactory results are achieved if the equations for $\dot{\gamma}_{1c}$ and $\dot{\gamma}_{2c}$ are substituted into the derivative of Eq. (59). Equation (59) also is used to express γ_1 and γ_2 in terms of β_1 and β_2. The result is

$$\dot{\alpha}_c = -A\, (k_1 \cos\alpha\, p_\epsilon - k_2 \sin\alpha\, q_\epsilon) \tag{63}$$

$$\dot{\beta}_{1c} = (k_6 B - k_3 C) \sin\alpha\, p_\epsilon + (k_7 B - k_4 C) \cos\alpha\, q_\epsilon - (k_8 D + k_5 A)\, r_\epsilon \tag{64}$$

$$\dot{\beta}_{2c} = (k_6 B + k_3 C) \sin\alpha\, p_\epsilon + (k_7 B + k_4 C) \cos\alpha\, q_\epsilon - (k_8 D - k_5 A)\, r_\epsilon \tag{65}$$

where

$$A = \mathrm{sgn}\left[\sin\frac{\beta_1 - \beta_2}{2} \cos\frac{\beta_1 + \beta_2}{2}\right]$$

$$B = \mathrm{sgn}\left[\sin\frac{\beta_1 - \beta_2}{2} \sin\frac{\beta_1 + \beta_2}{2}\right]$$

$$C = \mathrm{sgn}\left[\cos\frac{\beta_1 - \beta_2}{2} \cos\frac{\beta_1 + \beta_2}{2}\right]$$

$$D = \mathrm{sgn}\left[\cos\frac{\beta_1 - \beta_2}{2} \sin\frac{\beta_1 + \beta_2}{2}\right]$$

Inspection of Eqs. (63–65) will reveal that the determinant is nonzero for all $k_i > 0$. Digital simulation results will show that the forementioned control laws do give some improvement in the system transient response.

Thus two sets of gimbal control laws have been chosen, and several useful relations between the gains have been derived. The description of the precession motor dynamics will be deferred to the digital sigmulation section.

Control of Reaction Jets for Desaturation

It has been stated that the controller will be defined as saturated when λ is less than a predetermined small angle λ_0. Considering Fig. 3, λ easily is shown to satisfy the relation

$$\cos(\lambda/2) = (1/2^{1/2})\, [1 + \cos(\beta_1 + \beta_2)]^{1/2} \tag{66}$$

It is desired to pulse the reaction jets when $\lambda \leq \lambda_0$. Equation (66) then gives that

$$\cos(\beta_1 + \beta_2) \geq 2 \cos^2(\lambda_0/2) - 1 = \mathrm{const} \tag{67}$$

causes the jets to fire. The magnitude of the torque impulse to be applied about each vehicle axis is found by resolving the gyro angular momentum into vehicle coordinates and adding to each component the corresponding error in vehicle angular momentum.

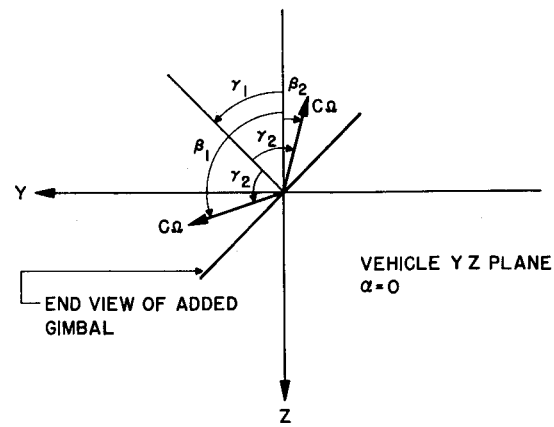

Fig. 5 Alternate mechanization of the gyro controller

Thus, to reduce angular rate errors to zero and increase λ from λ_0 to π rad,

$$T_X \cong p_\epsilon I_X - 2C\Omega \cos(\lambda_0/2) \sin\beta^* \sin\alpha \quad (68)$$

$$T_Y \cong q_\epsilon I_Y - 2C\Omega \cos(\lambda_0/2) \sin\beta^* \cos\alpha \quad (69)$$

$$T_Z \cong r_\epsilon I_Z + 2C\Omega \cos(\lambda_0/2) \cos\beta^* \quad (70)$$

The angle β^* is the angle that the resultant controller momentum vector $\bar{H}_g'$ makes with the $-Z$ axis and easily is shown to be

$$\beta^* = \tan^{-1}\left(\frac{\sin\beta_1 - \sin\beta_2}{\cos\beta_1 + \cos\beta_2}\right) \quad (71)$$

If λ_0 is sufficiently small, β^* can be approximated by β_1. The effect of Eqs. (68–70) is the following. When the controller saturates, the jets are activated, giving impulses about each vehicle axis as determined by Eqs. (68–70). As the result of the impulses, p_ϵ, q_ϵ, and r_ϵ change sign, and the gimbal motors increase λ from λ_0 toward π rad. If one neglects the fact that the equations are approximate and assumes that the gimbals reach the new positions instantaneously, the applied impulses are just sufficient to drive λ to π rad when p_ϵ, q_ϵ, and r_ϵ reach zero. However, the system still may be left with an attitude error.

Digital Simulation Study

Because of the nature of the control equations and the equations describing the dynamics of the gyros and vehicle, analysis of the complete system seems impossible except for certain special cases. Therefore, a digital simulation of an entire three-axis attitude control system, as illustrated by Fig. 4, has been completed. The simulation serves to demonstrate the effectiveness of the gyro controller and is an aid in selecting system parameters.

The equations of motion of the vehicle and the equations describing the motor and gimbal dynamics must be given to complete the system description. The vehicle equations are the usual Euler equations of motion:

$$\begin{aligned} I_X \dot{p} + (I_Z - I_Y)\, qr &= M_X \\ I_Y \dot{q} + (I_X - I_Z)\, rp &= M_Y \\ I_Z \dot{r} + (I_Y - I_X)\, pq &= M_Z \end{aligned} \quad (72)$$

where M_X, M_Y, M_Z are given by Eqs. (20–22), respectively. In the simulation, terms involving $(C - A)\dot{\alpha}$, $A\ \ddot{\beta}_1$, etc., are neglected in comparison to terms such as $I_a\ \ddot{\beta}_1$. In addition, ω_0 is assumed zero since the main objective is to study the system transient response. The equations

$$\begin{aligned} \dot{\psi}\cos\theta &= q\sin\phi + r\cos\phi \\ \dot{\theta} &= q\cos\phi - r\sin\phi \\ \dot{\phi} &= p + (q\sin\phi + r\cos\phi)\tan\theta \end{aligned} \quad (73)$$

complete the description of the vehicle motion.

As shown in Fig. 4, the angular rate commands are

$$\begin{aligned} p_c &= K_1(\phi_c - \phi) \\ q_c &= K_2(\theta_c - \theta) \\ r_c &= K_3(\psi_c - \psi) \end{aligned} \quad (74)$$

which are reasonable for small values of the Euler angles. The

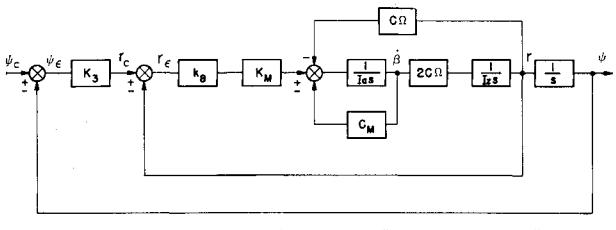

Fig. 6 Yaw axis attitude control system with gyros; special initial conditions

Table 1 System parameters

I_X	= 250 slug-ft²	λ_0	= 10°
I_Y	= 1300 slug-ft²	K_M	= 0.1304 ft-lb/rad/sec
I_Z	= 1500 slug-ft²	C_M	= 25 ft-lb/rad/sec
$C\Omega$	= 2.0 ft-lb-sec	I_a	= 1.0 slug-ft², referred to gimbal shaft (gear ratio = 500)
L_X	= 2.5 ft-lb		
L_Y	= 13.0 ft-lb	p_ϵ'	= $q_\epsilon' = r_\epsilon'$ = 0.005 rad/sec
L_Z	= 15.0 ft-lb		

Euler angles may be set equal to zero at $t = 0$ when studying the transient response without loss of generality, and, since the vehicle rates p, q, r are small, Eq. (74) is satisfactory.

Three servo motors with approximately 5-w capacity each are simulated to precess the gimbals. The linearized characteristic of each motor is

$$M = K_M \dot{\beta}_c - C_M \dot{\beta} \quad (75)$$

where M is the output torque, K_M the torque command constant, C_M the torque speed constant, and $\dot{\beta}$ the gimbal shaft rate. The equations describing the gimbal dynamics can be obtained by equating the torque delivered by each motor, as described by Eq. (75), to that required by the load, as described by the negative of Eq. (14) or (22). Thus, for one of the inner gimbals,

$$I_a \ddot{\beta}_1 + C_M \dot{\beta}_1 = K_M \dot{\beta}_{1c} - C\Omega\,[\dot{\alpha}\sin\beta_1 - (p\sin\alpha + q\cos\alpha)\cos\beta_1 - r\sin\beta_1] \quad (76)$$

with two similar equations for the remaining gimbals.

To illustrate the system in block diagram form, a special case is considered and presented in Fig. 6. The initial conditions are such that vehicle motion occurs only about the Z axis. Specifically, the initial conditions are those that led to Eqs. (23) and (24). In addition, $\phi_c = \theta_c = 0$, and ψ_c is small so that β_1 and β_2 do not depart appreciably from $\pi/2$. If $k_5 = k_8$, $\beta_1 = \beta_2$, and it can be shown that the linearized system is stable if

$$K_3 < [(C\Omega + k_8)\, C_M/k_8\, I_a] \quad (77)$$

An analysis of Fig. 6 is useful in that it serves as a starting point for determination of the k_i. The fixed system parameters used in the simulation are summarized in Table 1, where p_ϵ', q_ϵ', and r_ϵ' are the values of p_ϵ, q_ϵ, and r_ϵ, respectively, at which the reaction jets are activated. When the reaction jets for a particular vehicle axis are in operation, the corresponding terms in the gimbal control equations are set equal to zero.

To check the validity of the energy relation, Eq. (40), a series of runs was made with the angular rate control system. The initial conditions for the runs are the same as used for Fig. 6, except that $r_c = 0.002$ rad/sec. By varying k_5, one can vary the response time. The response time is defined as the time required for the system to reach and remain within 95% of the steady-state conditions. If one considers a flywheel system in which $I_Z/C_2 = 10^5$, 300 ft-lb energy is required to perform the maneuver under consideration.

In Fig. 7, the ratio $E_2/E_1 = 300/E_1$ is plotted as a function of the response time. The increase of E_2/E_1 with response time is as expected, since the peak rotor speed decreases, and hence less energy is expended in accelerating and decelerating the rotor. It should be mentioned that the energy required to maintain constant gyro wheel speed has been neglected.

For the remainder of the results to be presented, the gimbal control laws given by Eqs. (48, 50, and 51) are designated as set A, and those given by Eqs. (63–65) are designated as set B. In Table 2 the gains used are summarized, and the units of k_i are ft-lb/rad/sec because K_M, the motor torque command gain, is included. The parameters $K_1 = K_2 = K_3 = 0.2$ rad/sec/rad are common to both systems.

Figure 8 demonstrates the rate control system response to a step command in roll rate p, with perhaps the most difficult

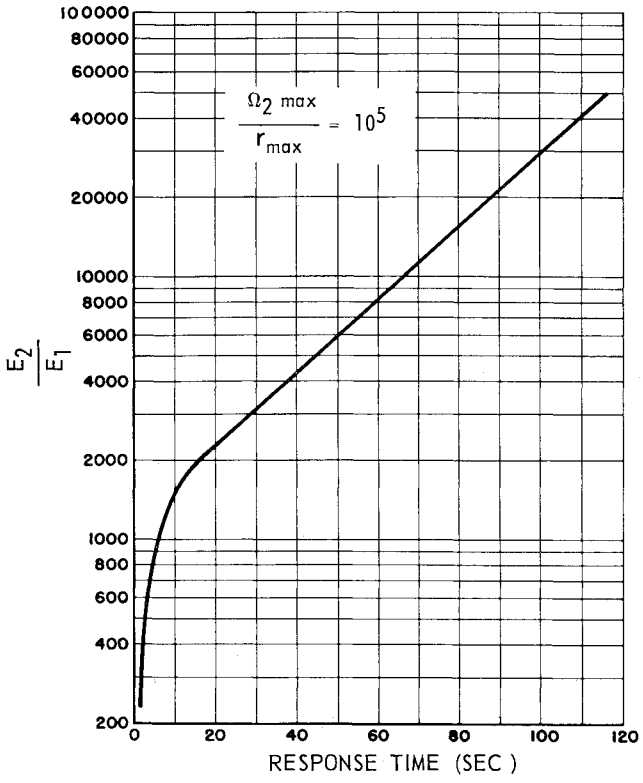

Fig. 7 Energy comparison for gyro and flywheel systems

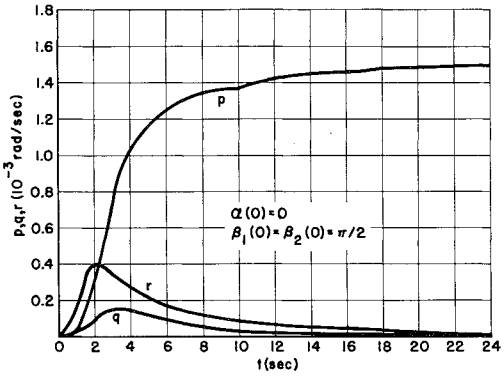

Fig. 8 Rate control system response for $p_c = 0.0015$ rad/sec; control equation A

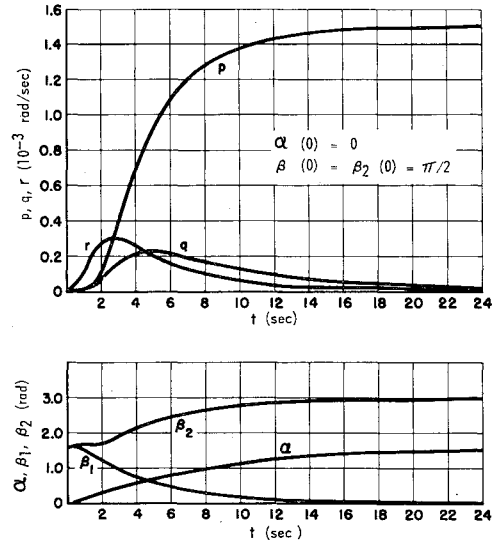

Fig. 9 Rate control system response for $p_c = 0.0015$ rad/sec; control equation B

Table 2 System gains

Set A	Set B
k_1 = 5000 ft-lb/rad/sec	k_1 = 2500 ft-lb/rad/sec
k_2 = 26,000 ft-lb/rad/sec	k_2 = 13,000 ft-lb/rad/sec
k_3 = 20,000 ft-lb/rad/sec	k_3 = 10,000 ft-lb/rad/sec
k_4 = 20,000 ft-lb/rad/sec	k_4 = 10,000 ft-lb/rad/sec
k_5 = 10,000 ft-lb/rad/sec	k_5 = 10,000 ft-lb/rad/sec
k_6 = 20,000 ft-lb/rad/sec	k_6 = 20,000 ft-lb/rad/sec
k_7 = 20,000 ft-lb/rad/sec	k_7 = 20,000 ft-lb/rad/sec
k_8 = 40,000 ft-lb/rad/sec	k_8 = 20,000 ft-lb/rad/sec

set of initial conditions which the system will encounter. The initial conditions are such that the plane defined by the two gyro spin axes is normal to the vehicle X axis at $t = 0$. Thus the outer gimbal must rotate through $\pi/2$ rad, and cross-coupling moments act about both the Y and the Z axes.

In Fig. 9 the rate control system response with control equations B is shown. The initial conditions are identical to those for Fig. 8. Some improvement in transient response is noted.

A large rate command applied to the X axis produces the results shown in Fig. 10. The reaction jets remain on until the rate error is reduced to 0.005 rad/sec, at which time the gyro controller assumes command. Again the initial conditions are $\alpha(0) = 0$, $\beta_1(0) = \beta_2(0) = \pi/2$.

For Fig. 11 simultaneous rate commands of 0.0015 rad/sec were applied to all three vehicle axes. Control equations A and initial conditions $\alpha(0) = 0$, $\beta_1(0) = \beta_2(0) = \pi/2$ apply.

As might be expected, control of the vehicle attitude is more difficult than control of its angular rate. When a change in attitude is desired, the gimbals must precess in such a fashion as to impart an angular velocity about the appropriate vehicle

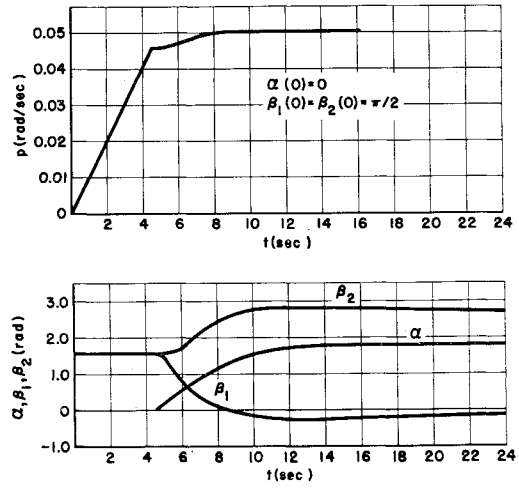

Fig. 10 Rate control system response for a large command, $p_c = 0.05$ rad/sec; control equation B

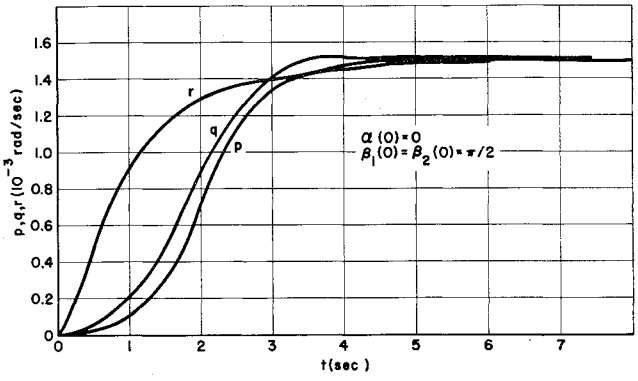

Fig. 11 Rate control system response for $p_c = q_c = r_c = 0.0015$ rad/sec; control equations A

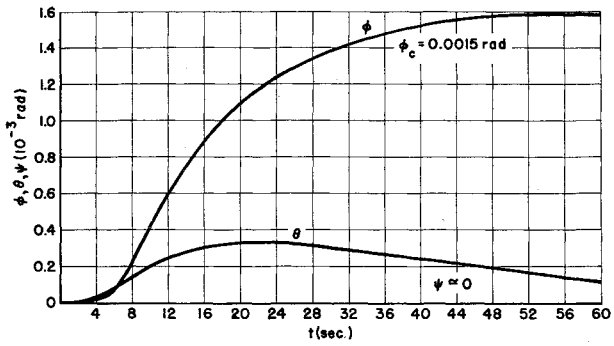

Fig. 12 Attitude control system response; control equations A

axes. Then, as the vehicle assumes the correct attitude, the vehicle rate must be reduced to zero. The gimbal orientation, of course, must be consistent at all times with the initial angular momentum of the system. For small vehicle reorientation angles this results in a final orientation of the gimbals which is essentially the same as that at the beginning of the maneuver.

If $\alpha(0) = 0$ and $\beta_1(0) = \beta_2(0) = \pi/2$ as before, a change in roll attitude ϕ requires that the outer gimbal precess through approximately $\pi/2$ rad and then back to nearly zero. In Fig. 12 the system response is shown for the forementioned initial conditions, control equations A, and $\phi_c = 0.0015$ rad. The values of K_1, K_2, K_3 seem to be critical for this case. As they are increased above about 0.5, the overshoot in attitude becomes appreciable. For the system gains chosen, control equations B give a response almost identical to that shown in Fig. 12. Further study is required to determine the relative merits of the two sets.

Conclusions

A gyro momentum exchange device has been described which, for general application, probably contains the minimum number of wheels and gimbals. The cross-coupling between vehicle axes is somewhat greater than that with three separate single-axis controllers, but in most cases it should be tolerable. The gyro controller has been shown to be a very efficient device from an energy point of view. In addition, the motor size required for a given response time is greatly in favor of the gyro system over the flywheel system.

Control system synthesis is hindered by the fact that gimbal motion is not associated with a particular vehicle axis, thus requiring closely coupled control equations. In addition, the equations describing the motion of the gimbals are nonlinear. The possibility that more efficient control equations exist should be investigated, and methods of mechanizing the equations should be considered. The gyro controller possibly could operate as efficiently with different definitions of system error. For example, it may be possible to eliminate the vehicle angular rate measuring equipment. In any case, careful analysis will be required to uncover any possible system limit cycles that occur as the result of discontinuities or nonlinearities in the control equations.

References

[1] Cannon, R. H., Jr., "Some basic response relations for reaction-wheel attitude control," ARS J. **32**, 61–74 (1962).

[2] Ormsby, R. D. and Smith, M. C., "Capabilities and limitations of reaction spheres for attitude control," ARS J. **31**, 808–812 (1961).

[3] Haeussermann, W., "A comparison of actuation methods for attitude control of space vehicles," *Proceedings of the Manned Space Station Symposium* (Inst. Aerospace Sci., New York, 1960), pp. 267–274.

[4] White, J. S. and Hansen, Q. M., "Study of a satellite attitude control system using integrating gyros as torque sources," NASA TND-1073 (September 1961).

[5] Kennedy, H. B., 'Attitude control of space vehicles using gyro precession torques," *Ballistic Missile and Aerospace Technology* (Academic Press Inc., New York, 1961), Vol. II, pp. 153–183.

[6] Cannon, R. H., Jr., "Gyroscopic coupling in space vehicle attitude control systems," J. Basic Eng. **84D**, no. 1 (March 1962).

[7] Klass, P. J., "New gyro technique orients satellite," Aviation Week Space Technol. **76**, 68–73 (February 12, 1962).

[8] Roberson, R. E., "Gyroscopic control of satellite attitude," *Proceedings of the First Symposium (International) on Rockets and Astronautics* (1959), pp. 307–316.